coatings

MDPI

Article

Assessment of *Streptococcus Mutans* Adhesion to the Surface of Biomimetically-Modified Orthodontic Archwires

Santiago Arango-Santander [1,*], Carolina Gonzalez [2], Anizac Aguilar [2], Alejandro Cano [2], Sergio Castro [2], Juliana Sanchez-Garzon [2,3] and John Franco [2,4]

1 GIOM Group, Faculty of Dentistry, Universidad Cooperativa de Colombia, Envigado 055422, Colombia
2 Faculty of Dentistry, Universidad Cooperativa de Colombia, Envigado 055422, Colombia; carolina.gonzalezve@campusucc.edu.co (C.G.); anizac.aguilar@campusucc.edu.co (A.A.); alejandro.canom@campusucc.edu.co (A.C.); sergioa.castro@campusucc.edu.co (S.C.); juliana.sanchezga@campusucc.edu.co (J.S.-G.); john.francoa@campusucc.edu.co (J.F.)
3 CES University, Medellín 050021, Colombia
4 Universidad de Antioquia, Medellín 050010, Colombia
* Correspondence: santiago.arango@campusucc.edu.co; Tel.: +57-4-4446065

Received: 30 December 2019; Accepted: 3 February 2020; Published: 26 February 2020

Abstract: Bacterial adhesion and biofilm formation on the surfaces of dental and orthodontic biomaterials is primary responsible for oral diseases and biomaterial deterioration. A number of alternatives to reduce bacterial adhesion to biomaterials, including surface modification using a variety of techniques, has been proposed. Even though surface modification has demonstrated a reduction in bacterial adhesion, information on surface modification and biomimetics to reduce bacterial adhesion to a surface is scarce. Therefore, the main objective of this work was to assess bacterial adhesion to orthodontic archwires that were modified following a biomimetic approach. The sample consisted of 0.017 × 0.025, 10 mm-long 316L stainless steel and NiTi orthodontic archwire fragments. For soft lithography, a polydimethylsiloxane (PDMS) stamp was obtained after duplicating the surface of *Colocasia esculenta* (L) Schott leaves. Topography transfer to the archwires was performed using silica sol. Surface hydrophobicity was assessed by contact angle and surface roughness by atomic force microscopy. Bacterial adhesion was evaluated using *Streptococcus mutans*. The topography of the *Colocasia esculenta* (L) Schott leaf was successfully transferred to the surface of the archwires. Contact angle and roughness between modified and unmodified archwire surfaces was statistically significant. A statistically significant reduction in *Streptococcus mutans* adhesion to modified archwires was also observed.

Keywords: bacterial adhesion; soft lithography; biomimetics; surface modification

1. Introduction

Many elements are involved in the orthodontic treatment of dental malocclusions. Stainless steel and titanium alloys are essential to manufacture brackets and archwires. These alloys have been widely used due to their outstanding mechanical properties and high corrosion resistance [1,2]. In the oral cavity, alloys are exposed to saliva, biological fluids and bacteria, which ultimately may cause deterioration and corrosion [3]. The presence of bacteria is a fundamental event that leads to metal corrosion and degradation as bacteria first adhere to a surface and biofilm will eventually be formed [4]. Biofilm formation has been largely associated with treatment failure in the biomedical field [5], including orthodontics [6]. Corrosive degradation might occur in biometals when bacteria adhere to the surface and may absorb and metabolize the metal or they might increase the acidity level

around the biometal by reducing the pH, which leads to metal corrosion [1]. In orthodontic alloys, this corrosion might affect the biocompatibility and performance of the appliance, which will lead to treatment failure or an increase in treatment time [3,6]. However, titanium alloys are among the most resistant to corrosion caused by oral microorganisms [7]. Furthermore, adhesion and colonization of bacteria on dental biomaterial surfaces might lead to the onset of different conditions, namely secondary caries or periodontal disease as the two most relevant [8].

Different alternatives have been proposed to reduce bacterial adhesion to the surface of biomaterials. Among such alternatives, physical surface modifications, including roughening of zirconia surfaces [9] or modification of the topography of materials to observe cellular [10,11] or bacterial behavior [12], have received attention in the last years.

An array of direct and indirect techniques to modify the surface of a material have been evaluated, including soft lithography, photolithography or dip-pen nanolithography [13–15]. Soft lithography is a set of easy-to-use and low-cost techniques that allows surface modification at nano and micro scales. This technique is based on the construction of a stamp, typically made of polydimethylsiloxane (PDMS), to duplicate the topography of one surface and then transfer it to another surface of interest [16]. Traditionally, photolithography has been used to fabricate the master model that is duplicated with soft lithographic techniques [17–21]. However, photolithography presents some disadvantages, including high costs, no control over the surface chemistry and impossibility to be applied on non-planar surfaces [22]. Therefore, alternatives have been investigated to fabricate the master model [12].

In this regard, biomimetics may be presented as an alternative to photolithography since nature has created master models on plant or animal surfaces over millions of years of evolution to resolve its own problems. Humans have been exploring such master models to use them in industrial and biomedical applications, among many others [23,24]. Chung et al. [25] used the topography of the shark skin as a master model to assess bacterial adhesion, while Bixler et al. [26] created a bio-inspired, anti-fouling surface based on the topography of rice leaves and butterfly wings. A well-known example of biomimetics is the lotus effect. In this effect, adhesion to the surface of the *Lotus* leaf is impaired by physical arrays and chemical processes that lead to the impossibility of dust or other agents to remain on the surface as they are washed off by water. This phenomenon is known as self-cleaning [24,27] and is related to the hydrophobicity of the surface.

Many plants and leaves that show the super hydrophobicity and self-cleaning effects are reported in the literature. Among them, *Colocasia esculenta* (L) Schott, a plant from tropical Asia but found in tropical and sub-tropical areas around the world [28], has been recognized as having super hydrophobic leaves. Surface hydrophobicity is measured using the contact angle (CA) measurement, which is the angle that forms between a drop of liquid and the solid surface. Depending on the CA, surfaces may be classified as super hydrophilic (CA<10°), hydrophilic (CA >10° but < 90°), hydrophobic (CA >90° but < 150°) and super hydrophobic (CA>150°) [24]. According to Neinhuis and Barthlott [29], *C. esculenta* shows a contact angle value of 164°, which places it in the super hydrophobic category. Hüger et al. [30] and Bhushan and Jung [31] demonstrated that the leaf of this plant presents a hierarchical structure that is responsible for the super hydrophobic behavior and optimal self-cleaning properties. In addition, these authors established that the leaf is also covered by wax, which in combination with the surface roughness, provides the super hydrophobic characteristic.

Current research in surface modification to reduce bacterial adhesion has produced interesting results. Chung et al. [25] modified the surface of PDMS and demonstrated a reduction in the adhesion of *Staphylococcus aureus.* Vasudevan et al. [32] compared *Staphylococcus cloacae* adhesion to modified vs. unmodified surfaces and found a higher rate of biofilm formation on the unmodified (50%) vs. the modified surface (<20%). Hochbaum y Aizenberg [33] concluded that physically modified surfaces reduced bacterial adhesion and Xu y Siedlecki [34] compared *Staphylococcus epidermidis* and *S. aureus* adhesion to polyurethane urea and a reduction in biofilm formation on the modified surface was observed. However, surface modification approaches are scarce in the fields of dentistry and orthodontics, particularly following a biomimetic approach. Moreover, to the best of our knowledge,

the use of *C. esculenta* as a master model for surface modification in the biomedical field has not been investigated. Therefore, the objective of this work was to assess bacterial adhesion to the surface of modified stainless steel and NiTi orthodontic archwires following a biomimetic approach.

2. Materials and Methods

2.1. Substrate

0.017 × 0.025 in, 10 mm-long 316L stainless steel and NiTi orthodontic archwire fragments (ORMCO, Orange, CA, USA) were used. The archwire fragments of the aforementioned dimensions were sequentially cleaned, following a protocol established by our group [12,35], using surfactant, acetone (99.8% v/v, Merck Millipore, Burlington, MA, USA), distilled water (Protokimica, Medellin, Colombia), and absolute ethanol (99% v/v, Merck Millipore, Burlington, MA, USA) for 8 min each in an ultrasound bath and let dry in air.

2.2. Silica sol Synthesis

The one-stage sol-gel method was used to synthetize the silica sol [36]. Tetraethylorthosilicate (TEOS) and methyltriethoxysilane (MTES) (ABCR GmbH & Co., Karlsruhe, Germany) were used as silica precursors for the hybrid sol, 0.1N nitric acid (Merck Millipore, Burlington, MA, USA) and acetic acid (glacial, 100% v/v, Merck Millipore, Burlington, MA, USA) were used as catalysts, and absolute ethanol (99.9% v/v, Merck Millipore, Burlington, MA, USA) was used as solvent. The obtained final concentration of SiO_2 was 18 gL^{-1}.

2.3. Surface Modification

For the experimental groups, the *C. esculenta* leaf was cut in segments of 5.0 cm in diameter avoiding the central vein. Leaf fragments were placed at the bottom of a silicone container, the lamina of the leaf facing upward. Polydimethylsiloxane (PDMS) (Silastic T-2, Dow Corning Corporation, Midland, MI, USA) was used to duplicate the surface of the leaf. PDMS was prepared according to the manufacturer, poured to cover the leaf and cured for 24 h. Then, the leaf was carefully removed from the surface and the PDMS stamp was inspected to verify its integrity before completing polymerization at 80 °C for 3 h. The PDMS was used as a microstamp to transfer SiO_2 to one archwire surface. One of the 0.025 in surfaces was selected due to the higher area. 2 µL of the silica sol were deposited on the archwire surface, a microstamp was placed over the drop applying mild pressure, and the sol was allowed to gel for 4 h at RT. Then, the PDMS stamp was removed, and the archwire with the transferred pattern was heat treated in a furnace at 450 °C for 30 min [12]. Two experimental groups resulted: SS316L and NiTi modified wires (SS316L_e and NiTi_e). The control groups consisted of cleaned, unmodified 316L stainless steel and NiTi orthodontic archwire fragments of the same dimensions as the experimental groups (SS316L_c and NiTi_c).

2.4. Surface Characterization

The lamina of the *C. esculenta* Schott leaf and the archwire fragments from the experimental and control groups were characterized through atomic force microscopy (AFM) (Nanosurf Easyscan 2, Nanosurf AG, Liestal, Switzerland). For AFM acquisition, a NCLR tip (Nanosensors™, Neuchâtel, Switzerland) in tapping mode at a constant force of 48 N/m was used. Images were processed using software AxioVision (V 4.9.1.0, Carl Zeiss Microscopy GmbH, Jena, Germany), software Image J 1.51 J (Laboratory for Optical and Computational Instrumentation, University of Winsconsin, Madison, WI, USA) [37], and software WSxM 5.0 (Nanotec Electrónica and New Microscopy Laboratory, Madrid, Spain) [38]. 10 AFM images of 50 µm × 50 µm were used to measure surface roughness and the arithmetic average of the roughness profile (Ra) was calculated using software for AFM analysis (Gwyddion 2.34, Department of Nanometrology, Czech Metrology Institute, Brno, Czech Republic). To measure surface hydrophobicity, the sessile drop method was applied on 10 random fragments

from each group. The contact angle images were attained using a camera (Canon EOS Rebel XS, Tokyo, Japan) and a macrolens (105mmF2.8 EX DG OS, Sigma, Ronkonkoma, NY, USA). Contact angle values were obtained using software AxioVision.

2.5. Bacterial Adhesion

Adhesion of *Streptococcus mutans* (ATCC 25175, Microbiologics, St. Cloud, MN, USA) to experimental and control surfaces was evaluated following a protocol previously published by our group [12,35]. *S. mutans* were grown in Heart-Brain Infusion (BHI) agar (Scharlab S.L., Barcelona, Spain) supplemented with 0.2 U/mL bacitracin (Sigma Fluka, St. Louis, MO, USA) for 24 h at 37° ± 1° C. Then, they were cultured in a solution of peptone water at 37° ± 1°C for 24 h. After centrifugation of the bacterial solution, the supernatant was discarded, followed by resuspension of the bacterial pellet in peptone water. The nephelometric turbidity unit (NTU)) (based on a calibration curve of NTU vs CFU/mL) was used to obtain a 10^{-7} CFUs/mL concentration. 40 archwire fragments from control and experimental groups (10 archwire fragments per group) were placed in wells of 24-well non-treated polystyrene plates (Costar, Corning Inc., NY, USA), and 500 µL of bacterial solution was added to each well. At the bottom of each well, a rubber matrix was placed and the respective modified archwire was embedded leaving only the modified surface exposed to the bacterial solution. In the case of unmodified archwires, the fragment was also embedded leaving only one 0.025 in surface exposed to the bacterial solution. This procedure was performed to ensure that bacteria could only adhere to the modified surface, or one surface in the case of unmodified archwires, and not to untreated surfaces.

Polystyrene plates were incubated at 37° ± 1° C for 2 and 6 h. After each incubation time, archwires were removed from the wells and washed three times with 500 µL of 0.9% saline solution (Corpaul, Medellin, Colombia) to remove non-adherent bacteria. Archwire fragments from control and experimental surfaces were then subjected to sonication at 50% power (Qsonica 125, Newtown, CT, USA) in 10 mL of 0.9% saline solution for 3 seconds. The sonicated solutions were serially diluted and 10 µL from each dilution were cultured in BHI agar in triplicate following the drop plate method [39]. Culture plates were incubated at 37° ± 1°C for 48 h, followed by counting the colony-forming units (CFUs). This process was repeated in triplicate during different periods.

2.6. Statistical Analysis

A univariate analysis to describe roughness, contact angle and bacterial adhesion by estimation of central tendency and dispersion was performed. Results are presented as the mean ± standard deviation (SD). The one-way ANOVA test with post hoc Tukey method was used for comparison among groups after previous verification of the assumption of normality and homogeneity of variances through the Shapiro Wilk and Levene tests, respectively. Values of $p < 0.05$ were considered statistically significant. Software SPSS (V. 25) (IBM Corp., Armonk, NY, USA) and GraphPad Prism 8.3.0 (GraphPad Software, San Diego, CA, USA) were used for statistical analyses.

3. Results

3.1. Surface Modification

Figure 1 shows 100 µm × 100 µm (a) and 50 µm × 50 µm (b) AFM images of the lamina of the *C. esculenta* leaf. Figure 2 shows 50 µm × 50 µm AFM images of control stainless steel 316L (a) and nickel-titanium (b) surfaces. In addition, successful transference of the *C. esculenta* topography to the surface of stainless steel (c) and NiTi (d) orthodontic archwires is shown.

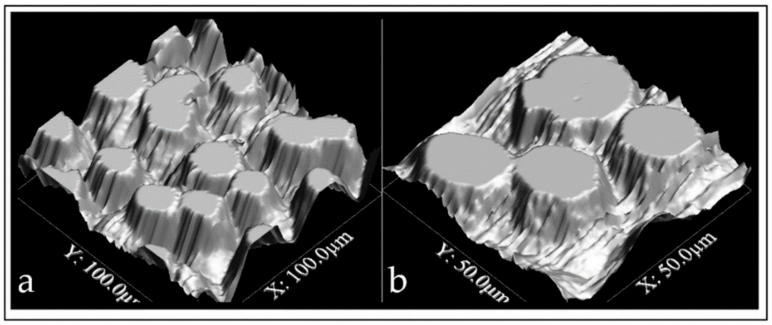

Figure 1. AFM image of the *C. esculenta* Schott leaf at 100 × 100 µm (**a**) and 50 × 50µm (**b**).

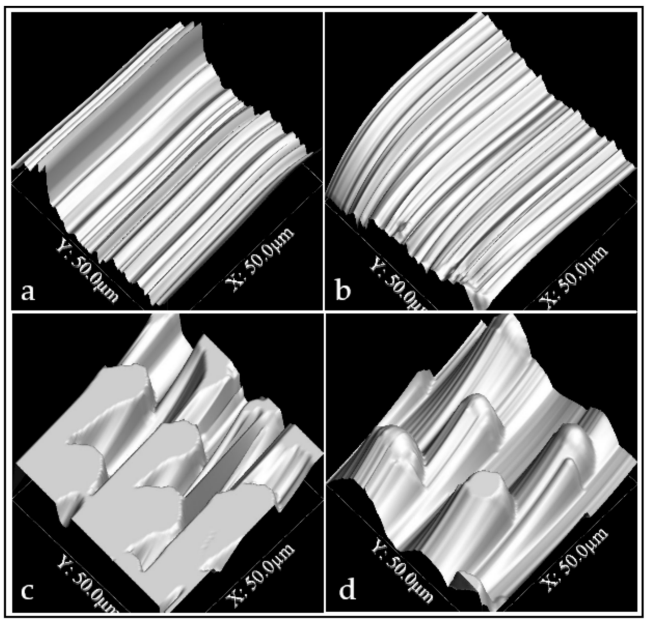

Figure 2. AFM images of control SS316L (**a**) and NiTi (**b**). Transference of the topography from *C. esculenta* to SS316L (**c**) and NiTi (**d**) were successful.

3.2. Surface Characterization

Contact angle measurements for control and experimental groups for both substrates are shown in Figure 3a. The most hydrophobic surface was the experimental NiTi (CA=129.4 ± 4.8°) and the least hydrophobic surface was the control 316L (CA=76.8 ± 6.9°). The difference between control and experimental surfaces for both substrates was statistically significant (P<0.0001), as well as the difference between both substrates (P<0.0001). The contact angle value of the *C. esculenta* Schott leaf was 131.2 ± 7.1°.

Regarding roughness measurements (Ra) for control and experimental groups for both substrates, results are shown in Figure 3b. The roughest surface was the experimental NiTi (Ra=142.3 ± 31.9 nm) and the smoothest was the control NiTi (Ra=34.1 ± 4.9 nm). The difference between SS316L_c and NiTi_c was statistically significant (P=0.0005), as well as the difference between SS316L_e and NiTi_c (P=<0.0001) and NiTi_c and NiTi_e (P<0.0001). The Ra of the *C. esculenta* Schott leaf was 270.6 ± 37.0 nm. Table 1 summarizes the results of contact angle and roughness values for the different groups.

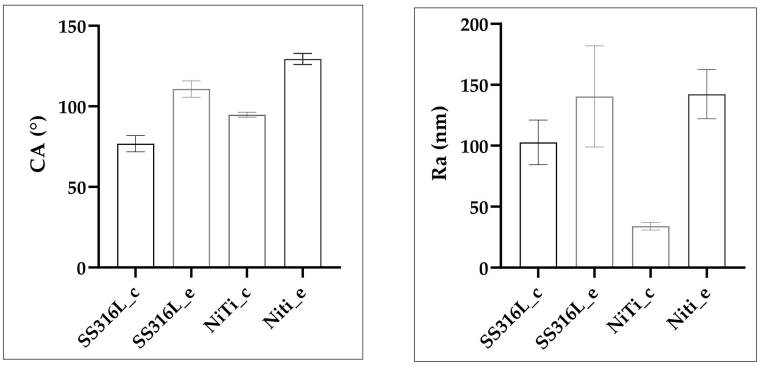

(**a**) (**b**)

Figure 3. Contact angle (**a**) and Ra (**b**) measurements of experimental and control surfaces.

Table 1. Values for contact angle (CA) and roughness (Ra).

Group	CA (°)					Ra (nm)				
	Mean	SD	Min	Median	Max	Mean	SD	Min	Median	Max
SS316L_c	76.8	6.9	64.0	79.5	83.0	102.8	28.7	64.0	100.5	162.0
SS316L_e	110.8	7.1	96.0	113.5	118.0	140.4	65.2	54.0	134.0	251.0
NiTi_c	94.9	2.2	90.5	95.5	97.5	34.1	4.9	29.2	31.7	42.8
NiTi_e	129.4	4.8	120.2	130.8	135.4	142.3	31.9	119.9	125.1	204.5

3.3. Bacterial Adhesion

S. mutans was allowed to adhere to the four surfaces during the evaluated periods. The highest adhesion of *S. mutans* was to the SS316L_c surface, followed by adhesion to the NiTi_c surface. The difference in adhesion between both control surfaces was statistically significant (P=0.0242). The SS316L_e surface showed the lowest adhesion and no statistically significant difference was found at 2 and 6h. However, statistically significant differences were found between SS316L_e vs SS316L_c, SS316L_c vs NiTi_e, SS316L_e vs NiTi_c and NiTi_c vs NiTi_e (P=0.0015; 0.0024;0.0161 and 0.0369, respectively) The NiTi_e surface showed the second lowest adhesion and there was no statistically significant difference in time. The difference in adhesion to both experimental surfaces was not statistically significant (P = 0.6477, Figure 4). Table 2 summarizes the values of *S. mutans* adhesion to experimental and control surfaces at the evaluated times.

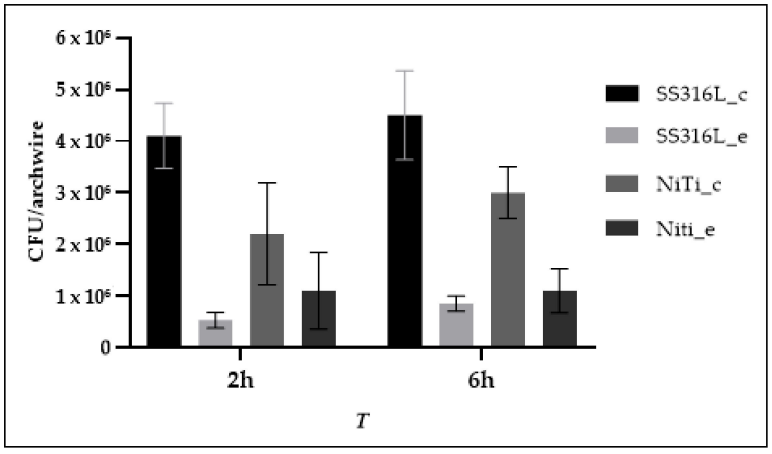

Figure 4. *S. mutans* adhesion to control and experimental surfaces at 2 and 6 hours.

Table 2. Values of *S. mutans* adhesion to control an experimental surfaces at the evaluated times.

Group	2h					6h				
	Mean	SD	Min	Median	Max	Mean	SD	Min	Median	Max
SS316L_c	4.1×10^6	6.3×10^5	3.4×10^6	4.2×10^6	5.0×10^6	4.5×10^6	8.6×10^5	3.2×10^6	4.6×10^6	5.6×10^6
SS316L_e	5.3×10^5	1.5×10^5	3.5×10^5	5.0×10^5	7.5×10^5	8.5×10^5	1.5×10^5	6.5×10^5	8.0×10^5	1.0×10^6
NiTi_c	2.2×10^6	9.9×10^5	1.4×10^6	1.9×10^6	3.8×10^6	3.0×10^6	5.0×10^5	2.3×10^6	3.0×10^6	3.6×10^6
NiTi_e	1.1×10^6	7.4×10^5	3.0×10^5	9.0×10^5	2.3×10^6	1.1×10^6	4.3×10^5	3.5×10^5	1.3×10^6	1.5×10^6

4. Discussion

Bacterial adhesion to a surface is a dynamic process and many variables related to the surface of the material and the bacterial species are involved. In orthodontics, bacterial adhesion and colonization have also been related to bracket presence and position [40], ligature method [41] and archwire material [42].

In the current work, surface characterization showed an increase in hydrophobicity on both substrates after surface modification was performed, which is in agreement with other results reported in the literature [12,43,44]. SS 316L modified surfaces showed an average of 110.8° in the contact angle measurement, while modified NiTi surfaces showed an average of 129.4° in the current work. Yang et al. [43] found contact angles in excess of 120° after using TEOS and MTES as silica precursors. Such angles depended on the morphology of the silica coatings and surface chemistry of the materials. Our previous work found an increase in the hydrophobicity of SS after modifying the surface using the same TEOS:MTES ratio used in the current work (57° to 87°), which are higher than the angles found in the present work, especially for the modified SS surface [12]. Other authors, including Santos et al. [45], Hosseinalipour et al. [44] and Wang et al. [46], have reported an increase in hydrophobicity. Wang et al. [46] demonstrated that an increase in the TEOS:MTES ratio increases hydrophobicity. They reported a contact angle value of 85° for a TEOS:MTES ratio similar to the current work. According to Wang et al. [46], such increase in surface hydrophobicity may be explained by the amount of methyl groups that might reduce the ability of the surface to absorb water. An additional explanation for this increase in surface hydrophobicity is that when roughness is created on a surface at the micro and nano scales, the water-air interface on a drop of liquid laying on such surface is enlarged and the capillary forces between the drop and the solid surface are reduced, which makes the drop take a spherical shape [23,47]. Nonetheless, the increase in hydrophobicity in this work appears to be related to the presence of silica on the modified surfaces rather than the presence of the features transferred from the *C. esculenta* leaf since its contact angle measurement was higher than that of the modified surfaces (131.2±7.1°), which is in agreement with the results of Burton and Bhushan [48]. This phenomenon may be explained by two facts: the leaf of *C. esculenta* has a hierarchical structure that provides pockets of air that lead to a high hydrophobicity [49] and the presence of a wax coating that covers the lamina of the leaf [48]. The transferring process used in the current investigation could not transfer the wax coating and only the external surface of the leaf could be copied and transferred, therefore, the complete hierarchical structure could not be transferred to the experimental surfaces.

Roughness was increased after modifying both substrates. SS 316L showed a higher increase in roughness than NiTi after modification. This increase in roughness from as-received to modified surfaces is in agreement with our previous work [12]. These results were expected since the patterns from *C. esculenta* showed a more voluminous topography that increased the roughness of the otherwise smooth untreated SS 316L and NiTi surfaces. Kim et al. [50] assessed the roughness of several orthodontic archwires and found a similar Ra for SS, even though they analyzed a different type of SS, and a higher Ra for the NiTi archwires. The leaf of *C. esculenta* showed higher roughness than the modified surfaces, which may be explained by the fact that a natural surface such as *C. esculenta´*s is not homogeneous since the hierarchical structures might have different heights.

Bacterial adhesion to the surface showed a reduction that had been observed in our previous work [12]. The work of Satou et al. [51] showed that the bacterial surface of *Streptococcus mutans* is rather

hydrophilic and they also observed that hydrophilic bacteria show higher adhesion to hydrophilic surfaces. In the current work, the observed reduction in *S. mutans* adhesion might be explained by the combination of a higher hydrophobicity from the silica and the presence of surface features from the *C. esculenta*, which might disrupt the way this bacterial species arrange on the surface, since the modified surfaces showed lower bacterial adhesion.

The relation between bacterial adhesion and surface roughness is not as clear. Kim et al. [50] suggested that surface tension plays a more significant role in bacterial adhesion than surface roughness. Hydrophobicity is influenced by roughness, but changes in the Ra should be larger than 0.1µm for the effect to be exhibited, as suggested by Busscher et al. [52]. The difference in the current work for SS 316L and NiTi was under 0.1µm, so roughness did not seem to play an important role for the increase in hydrophobicity. Therefore, the most likely explanation for the increase in hydrophobicity is the presence of the methyl groups as explained. According to this suggestion [50], roughness was not the most important factor for bacterial adhesion, since the smoothest surfaces showed higher bacterial adhesion. Therefore, the presence of the features copied from *C. esculenta* and the increase in hydrophobicity played the predominant roles for reduction of *S. mutans* adhesion to these surfaces.

The results of the current work showed a reduction of around 87% in *S. mutans* adhesion to SS 316L at 2 h and 81% at 6 h and around 50% at 2 h and 66% at 6 h on NiTi. These results are in agreement with the results of Chung et al. [25], who showed an 87% reduction in the adhesion of *S. aureus* at 14 days and May et al. [53], who found a 95% to 99% reduction in adhesion by different bacterial species. Our previous work found a 95% reduction in *S. mutans* adhesion to modified stainless steel plates [12]. These results are relevant for a short-time study and demonstrate that reduction of bacterial adhesion might be obtained using different substrates.

5. Conclusions and Considerations

Within the limitations of this work, the results showed a reduction in adhesion of *S. mutans* to modified stainless steel and nickel-titanium surfaces in a short-time study. These results are promising to consider biomimetics as an alternative approach to fabricate surfaces with antibacterial properties in the biomedical field. Limitations included the use of a single bacterial species, chemical characterization of the *C. esculenta* leaf, mechanical characterization of the coatings and longer periods of evaluation. It is also important to consider that orthodontic archwires are commercially available in different sections and sizes, which might have an influence on the results. All of these limitations should be addressed in future works, including the evaluation of other natural surfaces.

Author Contributions: Conceptualization, S.A.-S.; Data curation, J.S.-G. and J.F.; Formal analysis, J.S.-G. and J.F.; Investigation, S.A.-S., C.G., A.A., A.C. and S.C.; Methodology, S.A.-S., C.G., A.A., A.C. and S.C.; Project administration, S.A.-S.; Supervision, S.A.-S. and J.S.-G.; Writing – original draft, S.A.-S., C.G., A.A., A.C. and S.C.; Writing – review & editing, S.A.-S., J.S.-G. and J.F. All authors have read and agreed to the published version of the manuscript.

Funding: This research was funded by CONADI (2439).

Acknowledgments: The authors would like to thank Ph.D. Claudia García from Universidad Nacional de Colombia for her assistance with the sol-gel method and M.Sc. Johanna Gutiérrez from Tecnoacademia for her assistance with the AFM.

Conflicts of Interest: The authors declare no conflict of interest.

References

1. Arango-Santander, S.; Ramírez-Vega, C. Titanio: Aspectos del material para uso en ortodoncia. *Rev. Nac. Odontol.* **2016**, *12*, 63–71. [CrossRef]
2. Arango Santander, S.; Luna Ossa, C.M. Stainless Steel: Material Facts for the Orthodontic Practitioner. *Rev. Nac. Odontol.* **2015**, *11*, 71–82. [CrossRef]

3. Bahije, L.; Benyahia, H.; El Hamzaoui, S.; Ebn Touhami, M.; Bengueddour, R.; Rerhrhaye, W.; Abdallaoui, F.; Zaoui, F. Behavior of NiTi in the presence of oral bacteria: Corrosion by Streptococcus mutans. *Int. Orthod.* **2011**, *9*, 110–119. [CrossRef] [PubMed]
4. Renner, L.D.; Weibel, D.B. Physicochemical regulation of biofilm formation. *MRS Bull.* **2011**, *36*, 347–355. [CrossRef] [PubMed]
5. Campoccia, D.; Montanaro, L.; Arciola, C.R. A review of the biomaterials technologies for infection-resistant surfaces. *Biomaterials* **2013**, *34*, 8533–8554. [CrossRef] [PubMed]
6. Patil, P.; Kharbanda, O.P.; Duggal, R.; Das, T.K.; Kalyanasundaram, D. Surface deterioration and elemental composition of retrieved orthodontic miniscrews. *Am. J. Orthod. Dentofac. Orthop.* **2015**, *147*, S88–S100. [CrossRef]
7. Mystkowska, J.; Niemirowicz-Laskowska, K.; Łysik, D.; Tokajuk, G.; Dąbrowski, J.R.; Bucki, R. The role of oral cavity biofilm on metallic biomaterial surface destruction–corrosion and friction aspects. *Int. J. Mol. Sci.* **2018**, *19*, 743. [CrossRef]
8. Øilo, M.; Bakken, V. Biofilm and dental biomaterials. *Materials (Basel)* **2015**, *8*, 2887–2900. [CrossRef]
9. Al Qahtani, W.M.S.; Schille, C.; Spintzyk, S.; Al Qahtani, M.S.A.; Engel, E.; Geis-Gerstorfer, J.; Rupp, F.; Scheideler, L. Effect of surface modification of zirconia on cell adhesion, metabolic activity and proliferation of human osteoblasts. *Biomed. Tech.* **2017**, *62*, 75–87. [CrossRef]
10. Carvalho, A.; Pelaez-Vargas, A.; Gallego-Perez, D.; Grenho, L.; Fernandes, M.H.; De Aza, A.H.; Ferraz, M.P.; Hansford, D.J.; Monteiro, F.J. Micropatterned silica thin films with nanohydroxyapatite micro-aggregates for guided tissue regeneration. *Dent. Mater.* **2012**, *28*, 1250–1260. [CrossRef]
11. Laranjeira, M.S.; Carvalho, Â.; Pelaez-Vargas, A.; Hansford, D.; Ferraz, M.P.; Coimbra, S.; Costa, E.; Santos-Silva, A.; Fernandes, M.H.; Monteiro, F.J. Modulation of human dermal microvascular endothelial cell and human gingival fibroblast behavior by micropatterned silica coating surfaces for zirconia dental implant applications. *Sci. Technol. Adv. Mater.* **2014**, *15*, 025001. [CrossRef] [PubMed]
12. Arango-Santander, S.; Pelaez-Vargas, A.; Freitas, S.C.; García, C. Surface Modification by Combination of Dip-Pen Nanolithography and Soft Lithography for Reduction of Bacterial Adhesion. *J. Nanotechnol.* **2018**, *2018*, 10. [CrossRef]
13. Biswas, A.; Bayer, I.S.; Biris, A.S.; Wang, T.; Dervishi, E.; Faupel, F. Advances in top-down and bottom-up surface nanofabrication: Techniques, applications & future prospects. *Adv. Colloid Interface Sci.* **2012**, *170*, 2–27. [PubMed]
14. Arango, S.; Peláez-Vargas, A.; García, C. Coating and surface treatments on orthodontic metallic materials. *Coatings* **2013**, *3*, 1–15. [CrossRef]
15. Weibel, D.B.; DiLuzio, W.R.; Whitesides, G.M. Microfabrication meets microbiology. *Nat. Rev. Microbiol.* **2007**, *5*, 209–218. [CrossRef]
16. Xia, Y.; Whitesides, G.M. Soft Lithography. *Angew. Chemie Int. Ed.* **1998**, *37*, 550–575. [CrossRef]
17. Butler, R.T.; Ferrell, N.J.; Hansford, D.J. Spatial and geometrical control of silicification using a patterned poly-l-lysine template. *Appl. Surf. Sci.* **2006**, *252*, 7337–7342. [CrossRef]
18. Pelaez-Vargas, A.; Gallego-Perez, D.; Fernandes, M.H.; Hansford, D.; Monteiro, F.J. Microstructured coatings to study the behavior of osteoblast-like cells on hard materials. *Bone* **2011**, *48* (supp.2), s106. [CrossRef]
19. Kitzmiller, J.; Beversdorf, D.; Hansford, D. Fabrication and testing of microelectrodes for small-field cortical surface recordings. *Biomed. Microdevices* **2006**, *8*, 81–85. [CrossRef]
20. Pelaez-Vargas, A.; Ferrel, N.; Fernandes, M.H.; Hansford, D.J.; Monteiro, F.J. Cellular Alignment Induction during Early In Vitro Culture Stages Using Micropatterned Glass Coatings Produced by Sol-Gel Process. *Key Eng Mater* **2009**, *396–398*, 303–306. [CrossRef]
21. Ferrell, N.; Woodard, J.; Hansford, D. Fabrication of polymer microstructures for MEMS: Sacrificial layer micromolding and patterned substrate micromolding. *Biomed. Microdevices* **2007**, *9*, 815–821. [CrossRef] [PubMed]
22. Tran, K.T.M.; Nguyen, T.D. Lithography-based methods to manufacture biomaterials at small scales. *J. Sci. Adv. Mater. Devices* **2017**, *2*, 1–14. [CrossRef]
23. Solga, A.; Cerman, Z.; Striffler, B.F.; Spaeth, M.; Barthlott, W. The dream of staying clean: Lotus and biomimetic surfaces. *Bioinspir Biomim* **2007**, *2*, S126–S134. [CrossRef] [PubMed]
24. Koch, K.; Barthlott, W. Superhydrophobic and superhydrophilic plant surfaces: An inspiration for biomimetic materials. *Philos. Trans. R. Soc. A Math. Phys. Eng. Sci.* **2009**, *367*, 1487–1509. [CrossRef]

25. Chung, K.K.; Schumacher, J.F.; Sampson, E.M.; Burne, R.A.; Antonelli, P.J.; Brennan, A.B. Impact of engineered surface microtopography on biofilm formation of *Staphylococcus aureus*. *Biointerphases* **2007**, *2*, 89–94. [CrossRef]
26. Bixler, G.D.; Theiss, A.; Bhushan, B.; Lee, S.C. Anti-fouling properties of microstructured surfaces bio-inspired by rice leaves and butterfly wings. *J. Colloid Interface Sci.* **2014**, *419*, 114–133. [CrossRef]
27. Bhadra, C.M.; Khanh Truong, V.; Pham, V.T.H.; Al Kobaisi, M.; Seniutinas, G.; Wang, J.Y.; Juodkazis, S.; Crawford, R.J.; Ivanova, E.P. Antibacterial titanium nano-patterned arrays inspired by dragonfly wings. *Sci. Rep.* **2015**, *18*, 16817. [CrossRef]
28. Lim, T.K. *Edible medicinal and non-medicinal plants. Modifed stems, roots, bulbs*; Springer: London, UK, 2015; Volume 12.
29. Neinhuis, C.; Barthlott, W. Characterization and distribution of water-repellent, self-cleaning plant surfaces. *Ann. Bot.* **1997**, *79*, 667–677. [CrossRef]
30. Hüger, E.; Rothe, H.; Frant, M.; Grohmann, S.; Hildebrand, G.; Liefeith, K. Atomic force microscopy and thermodynamics on taro, a self-cleaning plant leaf. *Appl. Phys. Lett.* **2009**, *95*, 033702. [CrossRef]
31. Bhushan, B.; Jung, Y.C. Wetting, adhesion and friction of superhydrophobic and hydrophilic leaves and fabricated micro/nanopatterned surfaces. *J. Phys. Condens. Matter* **2008**, *20*, 225010. [CrossRef]
32. Vasudevan, R.; Kennedy, A.J.; Merritt, M.; Crocker, F.H.; Baney, R.H. Microscale patterned surfaces reduce bacterial fouling-microscopic and theoretical analysis. *Colloids Surfaces B Biointerfaces* **2014**, *117*, 225–232. [CrossRef] [PubMed]
33. Hochbaum, A.I.; Aizenberg, J. Bacteria pattern spontaneously on periodic nanostructure arrays. *Nano Lett.* **2010**, *10*, 3717–3721. [CrossRef] [PubMed]
34. Xu, L.C.; Siedlecki, C.A. Submicron-textured biomaterial surface reduces staphylococcal bacterial adhesion and biofilm formation. *Acta Biomater.* **2012**, *8*, 72–81. [CrossRef]
35. Arango-Santander, S.; Pelaez-Vargas, A.; Freitas, S.C.; García, C. A novel approach to create an antibacterial surface using titanium dioxide and a combination of dip-pen nanolithography and soft lithography. *Sci. Rep.* **2018**, *8*, 15818. [CrossRef] [PubMed]
36. Durán, A.; Conde, A.; Gómez Coedo, A.; Dorado, T.; García, C.; Ceré, S. Sol-gel coatings for protection and bioactivation of metals used in orthopaedic devices. *J. Mater. Chem.* **2004**, *14*, 2282–2290. [CrossRef]
37. Schneider, C.A.; Rasband, W.S.; Eliceiri, K.W. NIH Image to ImageJ: 25 years of image analysis. *Nat. Methods* **2012**, *9*, 671–675. [CrossRef]
38. Horcas, I.; Fernández, R.; Gómez-Rodríguez, J.M.; Colchero, J.; Gómez-Herrero, J.; Baro, A.M. WSXM: A software for scanning probe microscopy and a tool for nanotechnology. *Rev. Sci. Instrum.* **2007**, *78*, 013705. [CrossRef]
39. Naghili, H.; Tajik, H.; Mardani, K.; Razavi Rouhani, S.M.; Ehsani, A.; Zare, P. Validation of drop plate technique for bacterial enumeration by parametric and nonparametric tests. *Vet. Res. forum an Int. Q. J.* **2013**, *4*, 179–183.
40. Sfondrini, M.F.; Debiaggi, M.; Zara, F.; Brerra, R.; Comelli, M.; Bianchi, M.; Pollone, S.R.; Scribante, A. Influence of lingual bracket position on microbial and periodontal parameters in vivo. *J Appl Oral Sci.* **2012**, *20*, 357–361. [CrossRef]
41. Türkkahraman, H.; Sayin, M.O.; Bozkurt, F.Y.; Yetkin, Z.; Kaya, S.; Onal, S. Archwire ligation techniques, microbial colonization, and periodontal status in orthodontically treated patients. *Angle Orthod.* **2005**, *75*, 231–236.
42. Hepyukselen, B.G.; Cesur, M.G. Comparison of the microbial flora from different orthodontic archwires using a cultivation method and PCR: A prospective study. *Orthod Craniofac Res.* **2019**, *22*, 354–360. [CrossRef] [PubMed]
43. Yang, H.; Pi, P.; Cai, Z.Q.; Wen, X.; Wang, X.; Cheng, J.; Yang, Z. Facile preparation of super-hydrophobic and super-oleophilic silica film on stainless steel mesh via sol-gel process. *Appl. Surf. Sci.* **2010**, *256*, 4095–4102. [CrossRef]
44. Hosseinalipour, S.M.; Ershad-langroudi, A.; Hayati, A.N.; Nabizade-Haghighi, A.M. Characterization of sol-gel coated 316L stainless steel for biomedical applications. *Prog. Org. Coatings* **2010**, *67*, 371–374. [CrossRef]

45. Santos, O.; Nylander, T.; Rosmaninho, R.; Rizzo, G.; Yiantsios, S.; Andritsos, N.; Karabelas, A.; Müller-Steinhagen, H.; Melo, L.; Boulangé-Petermann, L.; et al. Modified stainless steel surfaces targeted to reduce fouling - Surface characterization. *J. Food Eng.* **2004**, *64*, 63–79. [CrossRef]
46. Wang, M.; Wang, Y.; Chen, Y.; Gu, H. Improving endothelialization on 316L stainless steel through wettability controllable coating by sol-gel technology. *Appl. Surf. Sci.* **2013**, *268*, 73–78. [CrossRef]
47. Herminghaus, S. Roughness-induced non-wetting. *Europhys. Lett.* **2000**, *52*, 165. [CrossRef]
48. Burton, Z.; Bhushan, B. Surface characterization and adhesion and friction properties of hydrophobic leaf surfaces. *Ultramicroscopy* **2006**, *106*, 709–719. [CrossRef]
49. Grewal, H.S.; Cho, I.J.; Yoon, E.S. The role of bio-inspired hierarchical structures in wetting. *Bioinspiration Biomim.* **2015**, *10*, 026009. [CrossRef]
50. Kim, I.H.; Park, H.S.; Kim, Y.K.; Kim, K.H.; Kwon, T.Y. Comparative short-term in vitro analysis of mutans streptococci adhesion on esthetic, nickel-titanium, and stainless-steel arch wires. *Angle Orthod.* **2014**, *84*, 680–686. [CrossRef]
51. Satou, J.; Fukunaga, A.; Satou, N.; Shintani, H.; Okuda, K. Streptococcal Adherence on Various Restorative Materials. *J. Dent. Res.* **1988**, *67*, 588–591. [CrossRef]
52. Busscher, H.J.; van Pelt, A.W.J.; de Boer, P.; de Jong, H.P.; Arends, J. The effect of surface roughening of polymers on measured contact angles of liquids. *Colloids and Surfaces* **1984**, *9*, 319–331. [CrossRef]
53. May, R.M.; Hoffman, M.G.; Sogo, M.J.; Parker, A.E.; O'Toole, G.A.; Brennan, A.B.; Reddy, S.T. Micro-patterned surfaces reduce bacterial colonization and biofilm formation in vitro: Potential for enhancing endotracheal tube designs. *Clin. Transl. Med.* **2014**, *3*, 8. [CrossRef] [PubMed]